Carbohydrate Research 346 (2011) 753–758

Contents lists available at ScienceDirect

Carbohydrate Research

journal homepage: www.elsevier.com/locate/carres

Water soluble heptakis(6-deoxy-6-thio)cyclomaltoheptaose capped gold nanoparticles via metal vapour synthesis: NMR structural characterization and complexation properties

Gloria Uccello-Barretta [a,*], Claudio Evangelisti [a], Federica Balzano [a], Letizia Vanni [a], Federica Aiello [a], Laszlo Jicsinszky [b]

[a] Dipartimento di Chimica e Chimica Industriale, Università degli Studi di Pisa, via Risorgimento 35, I-56126 Pisa, Italy
[b] CYCLOLAB Ltd, Illatos út 7, 1097 Budapest, Hungary

ARTICLE INFO

Article history:
Received 24 November 2010
Received in revised form 27 January 2011
Accepted 1 February 2011
Available online 28 February 2011

Keywords:
NMR spectroscopy
Gold
Nanoparticles
Cyclodextrins
Inclusion compounds

ABSTRACT

The complexation of heptakis(6-deoxy-6-thio)cyclomaltoheptaose to gold nanoparticles prepared by using the Metal Vapour Synthesis (MVS) led to water soluble gold nanoaggregates, thermally stable at 25 °C. The role of gold concentration in the MVS-derived starting solution as well as of the cyclodextrin to gold molar ratio on the size of cyclodextrin-capped gold nanoparticles were investigated. The ability of cyclodextrin bonded to gold nanoparticles to include deoxycytidine was also probed in comparison with that of 1-thio-β-D-glucose sodium salt.

1. Introduction

The unique properties of metal nanoparticles (M-NPs) account for their widespread applications in material science, catalysis, and biomedicine.[1–5] Their biotechnological applications as artificial receptors, drug delivery systems, or biosensors mainly rely on the fine tuning of their sizes. Thus several interdisciplinary investigations have been addressed to the development of efficient and reproducible methods for controlling nanoparticles growth in a hydrophilic environment.

Among M-NPs, gold nanoparticles (Au-NPs) are endowed with considerable potential to be a biomedicine by virtue of their improved stability and their optical and electronic properties.[6–10]

The supramolecular aggregation of gold nanoparticles to host compounds such as the cyclodextrins gives the opportunity to conjugate their biosensing properties to drug transport and controlled release for developing new strategies of specific drug targeting. In view of such a kind of attractive application, the affinity of sulfur to gold has been already exploited by using chemical reduction methods[11–14] in order to obtain heptakis(6-deoxy-6-thio)cyclomaltoheptaose (β-CDSH) (Chart 1) capped gold nanoparticles, which are water soluble.

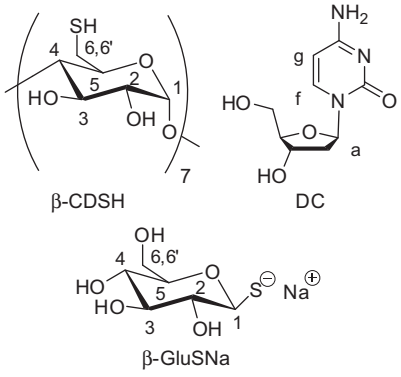

Chart 1.

Among the various preparative routes Metal Vapour Synthesis (MVS) provides a valuable way to obtain metal nanoparticles of tailored size.[15,16] The co-condensation of metal vapours with vapours of weakly stabilizing organic solvents on the cold walls (−196 °C) of a reactor affords solvent-stabilized metal nanoparticles (Solvated Metal Atoms, SMAs), which are soluble in excess of organic solvent. Metal nanoparticles obtained this way are very small (diameter <5 nm) and their sizes can be strictly controlled by means of selected experimental factors (i.e., kind of solvent, metal

* Corresponding author. Fax: +39 050 2219260.
E-mail address: gub@dcci.unipi.it (G. Uccello-Barretta).

0008-6215/$ - see front matter © 2011 Elsevier Ltd. All rights reserved.
doi:10.1016/j.carres.2011.02.001

concentration or keeping temperature) which affect the metal clustering processes.[17–19] Remarkable potentialities of MVS in exerting a fine tuning of nanoparticles sizes prompted us to exploit MVS technique in the preparation of water soluble Au-NPs stabilized by heptakis(6-deoxy-6-thio)cyclomaltoheptaose ($(Au)_n$/β-CDSH). The NMR DOSY (Diffusion-Ordered SpectroscopY) technique was employed as an effective, reliable and fast way to analyse the role of the total concentration of gold in SMA solutions as well as of the Au/β-CDSH molar ratio on nanoparticles sizes. The nature of supramolecular aggregation processes and the ability of $(Au)_n$/β-CDSH nanoaggregates to act as hosts for deoxycytidine (DC) (Chart 1) were also investigated by NMR in order to obtain some preliminary information on Au-NPs potentiality in the field of drug transport and release.

To mimic the effect of individual units of the cyclodextrin and thus assess the role played by the structural pre-organization of the cyclodextrin into supramolecular aggregation processes, we selected 1-thio-β-D-glucose sodium salt (β-GluSNa) (Chart 1) as a structural analogue of glucopyranose units of the host.

2. Results and discussion

2.1. Preparation of Au-NPs

In agreement with the previously reported procedure,[17] gold vapours (atoms) were co-condensed with vapours of acetone at the temperature of the liquid nitrogen. By further melting of the frozen gold/acetone matrix, a deep purple solution of solvated gold atoms was obtained that is stable at low temperature (−20 °C). The addition of β-CDSH to the Au/acetone solution gave a dark-purple powder of $(Au)_n$/β-CDSH which was insoluble in acetone and could be easily re-dissolved in water. Au/acetone SMAs with different Au concentration (0.4 mg Au/mL (LC) and 3.7 mg Au/mL (HC)) were prepared and these systems were used as starting materials for the preparation of β-CDSH-capped Au nanoparticles (Chart 2).

In all cases, the aggregates of $(Au)_n$/β-CDSH were easily separated from the eventual excess of β-CDSH by precipitation from the reaction mixture. Gold nanoparticles stabilized by β-GluSNa were prepared by a similar procedure (see Section 3).

2.2. Characterization of $(Au)_n$/β-CDSH NPs

The ^{1}H NMR (600 MHz, 25 °C, D_2O) spectrum of β-CDSH was in agreement with the presence of a symmetric structure where all primary sites were derivatized. During the time the spectrum of the cyclodextrin underwent relevant changes: each kind of glucopyranose proton produced a wide distribution of resonances which reflected the loss of symmetry. A significant decrease of the diffusion coefficient (D) was also detected in the DOSY maps: D value lowered from 2.4×10^{-10} m^2 s^{-1} in the freshly prepared sample to $1.7–1.8 \times 10^{-10}$ m^2 s^{-1} in the samples which were analysed at longer times, which was in agreement with the increase of the hydrodynamic radius (R_H) during the time. Eq. 1 gives the dependence of the diffusion coefficient on the hydrodynamic radius based on the Stokes–Einstein relationship, which strictly holds in the spherical approximation.

$$D = \frac{kT}{6\pi\eta R_H} \quad (1)$$

where k is the Boltzmann constant, T the absolute temperature and η is the solution viscosity.

A rough correlation of the diffusion coefficients to the molecular weights allowed us to establish that about a two to three-fold increase of the molecular weight occurred. Both the loss of proton isochrony and the increase of the molecular sizes pointed out the presence of oligomeric aggregates of the cyclodextrin due to the formation of disulfide bridges between primary groups of the cyclodextrin. Any further oligomerization was not detected at longer times.

The precipitates, which were formed as a consequence of the addition of the cyclodextrin to Au/acetone SMAs, were re-dissolved in D_2O and the corresponding limpid dark-purple solutions were stable at room temperature and could be analysed directly by NMR without any kind of preliminary manipulation. The significant changes detected in the spectral parameters of the cyclodextrin in $(Au)_n$/β-CDSH NPs relative to the pure cyclodextrin allowed us to investigate the nature of aggregation processes involved in the formation of D_2O soluble gold nanoparticles. The supramolecular assembly showed a marked dependence on the gold to cyclodextrin molar ratio and in some cases on the gold concentration in the starting Au/acetone SMA.

The ^{1}H NMR spectrum of the diluted preparations which contained gold 0.4 mg/mL in the presence of a large excess of cyclodextrin (molar ratio Au/β-CDSH = 1:5) resembled the spectrum of monomer cyclodextrin. A nearly complete isochrony of corresponding protons of the glucopyranose units was observed, but remarkable shifts of the signals (Table 1) were detected to be attributed to metal complexation. The major effects were detected for the higher frequency shifted methylene proton (H-6) belonging to the primary site and the proton H-4 which is located on the external surface of the cyclodextrin and is adjacent to the primary site.

The complexation of the metal to the thiol moieties of the cyclodextrin fully accounts for the complexation induced shifts of the cyclodextrin resonances.

The diffusion coefficient of 1.7×10^{-10} m^2 s^{-1} was measured, from which nanoparticles diameters about of 2.9 nm were calculated. On assuming a single shell of cyclodextrin units around Au-NPs, the average diameter of 1.3 nm was then estimated for gold core nanoaggregates. On the basis of the previously reported theoretical study,[20] it was possible to estimate that in our system about 80 atoms of gold were present in each nanoparticle and about the 75% of them were on the surface of the nanoparticle.

Interestingly, the behaviour of the residual acetone in the nanoparticles solution gave a further confirmation of the gold to cyclodextrin supramolecular assembly. As a matter of fact the residual acetone showed a diffusion coefficient of 7×10^{-10} m^2 s^{-1} which was remarkably lower than the value (15×10^{-10} m^2 s^{-1}) measured for the pure acetone in water. In the ROESY map, ROE effects were detected between acetone and the protons H-3–H-5 of the cyclodextrin which were located inside the cyclodextrin cavity. Reasonably the complexation of gold to the cyclodextrin drives the residual acetone inside the cyclodextrin cavity where a remarkable slowing down of its translational diffusion is produced.

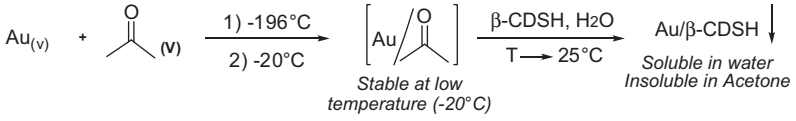

Chart 2.

Table 1
^{1}H NMR chemical shifts (δ, ppm, 600 MHz, D_2O, 25 °C) and complexation shifts $\Delta\delta$ ($\delta_{CDNPs} - \delta_{CD}$, ppm) of pure β-CDSH ($\delta_{CD}$) and of β-CDSH in $(Au)_n$/β-CDSH NPs (δ_{CDNPs}) obtained from 0.4 mg/mL of Au/acetone SMA (molar ratio Au/β-CDSH = 1:5)

Proton	δ_{CD}	δ_{CDNPs}	$\Delta\delta$
1	5.03	5.03	0.00
2	3.52	3.50	−0.02
3	3.83	3.80	−0.03
4	3.62	3.68	0.06
5	3.83	3.78	−0.05
6	2.94	2.86	−0.08
6′	2.83	2.81	−0.02

It is noteworthy that the NMR spectrum of the solution did not change with time, thus oxidation processes were not observed as in the case of pure cyclodextrin.

When the assembly of the gold nanoparticles and the cyclodextrin occurred in the presence of high Au/β-CDSH molar ratios (1:0.3), a remarkably different behaviour was found: less soluble nanoparticles were formed, which probably quickened the precipitation at very early stages of the metal nucleation. Accordingly, very small gold nanoparticles of 2.4 nm were formed and the ^{1}H NMR spectrum was very similar to that of the oxidized cyclodextrin, with the loss of symmetry. Thus, it would be concluded that excess of gold atoms favours the oxidation of cyclodextrin.

The behaviour observed at high Au/β-CDSH molar ratios was reproduced till the one to one molar ratio, that is, complexed oxidized cyclodextrin with formation of small nanoparticles. In all cases, very small nanoparticles sizes were obtained.

In order to study the effect of the gold concentration on the nanoparticles sizes distribution, we analysed the NMR spectra of the solutions obtained by adding different amounts of the cyclodextrin to a 3.7 mg/mL Au/acetone solution, that is, 10-fold more concentrated with respect to the cases just discussed. Four different molar ratios Au/β-CDSH were probed (1:5, 1:1, 1:0.3, 1:0.2) spanning from a molar excess of the cyclodextrin to a molar excess of gold atoms. The gold concentration did not affect the kind of cyclodextrin-to-gold assembly, which only depended on the gold to cyclodextrin molar ratio. As a matter of fact complexed monomer cyclodextrin was detected at high cyclodextrin/gold molar ratios, whereas oxidized cyclodextrin was present in the nanoparticles formed at high gold/cyclodextrin molar ratios. In the last case smaller nanoparticles of about 2.5 nm (Table 2) were found, irrespective of the total metal concentration. Only at high cyclodextrin/gold molar ratio, where the cyclodextrin was monomer, the nanoparticles sizes were sensitive to the concentration with an increase at higher gold concentrations and a wider sizes distribution, as revealed by the analysis of the diffusion coefficients (Table 2).

It is noteworthy that the pattern of intra-ring ROEs H-1–H-2 versus inter-ring ROEs H-1–H-4′ (the apex indicates the glucopyranose rings which is adjacent to the observed ones) was remarkably different in the solution containing the nanoparticles in comparison with the pure cyclodextrin. As shown in the Figure 1a, comparable effects were detected in the pure cyclodextrin, which

Table 2
Diffusion coefficients (D, $\times 10^{10}$ m^2 s^{-1}, D_2O, 600 MHz, 25 °C) of β-CDSH in $(Au)_n$/β-CDSH NPs obtained from the LC or HC Au/acetone SMA solutions at different Au/β-CDSH molar ratio and calculated hydrodynamic diameters (d_H, nm)

Au/β-CDSH	LC = 0.4 mg/mL Au		HC = 3.7 mg/mL Au	
	D	d_H	D	d_H
1:5	1.7	2.9	0.9 ÷ 1.6	5.4 ÷ 3.0
1:1	1.8	2.7	2.0	2.4
1:0.3	2.0	2.4	1.9	2.6
1:0.2			2.3	2.1

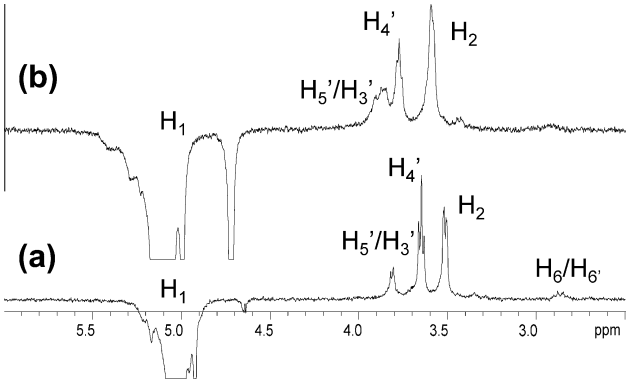

Figure 1. 1D ROESY (600 MHz, 25 °C, D_2O, mix = 0.3 s) spectra obtained by selective perturbation of H-1 nuclei of (a) β-CDSH and (b) $(Au)_n$/β-CDSH NPs (3.7 mg/mL Au/acetone SMA, molar ratio Au/β-CDSH = 1:5)

indicated nearly equal H-1–H-2 and H-1–H-4′ distances. In the solution containing $(Au)_n$/β-CDSH NPs (3.7 mg/mL Au/acetone SMA, molar ratio Au/β-CDSH = 1:5), the ROE H-1–H-2 was higher than the ROE H-1–H-4′ was (Fig. 1b), in agreement with the fact that the aggregation of the cyclodextrin to the gold nanoparticles caused a significant rotation of the glucopyranose rings about the glycosidic linkages, which turned the proton H-1 of one unit away from the proton H-4′ of the adjacent one.

2.3. NMR investigation of the complexation phenomena between deoxycytidine and $(Au)_n$/β-CDSH NPs

Nucleoside analogues are potential anticancer and/or antiviral agents, the solubility and transport of which could be improved by inclusion inside the cyclodextrin cavity. In view of such kind of applications we compared the ability of β-CDSH and $(Au)_n$/β-CDSH nanoparticles to include the deoxycytidine (DC). Complexation phenomena were detected by measuring the diffusion coefficients and the selective relaxation rates (R) of DC protons in the presence and in the absence of the cyclodextrin or cyclodextrin-capped gold nanoparticles.

The diffusion coefficients are very sensitive to complexation phenomena which slow down the translational diffusion of complexed species and, hence, bring about decreases of the diffusion parameters, which reflect the increase of the apparent sizes of complexed species with respect to uncomplexed ones (see Eq. 1). The selective relaxation rates (R) of protons of the ligand are more sensitive indicators of the binding than nonselective rates (R^{ns}) are. In fact, methods based on the determination of the selective relaxation rates take advantage of the favourable dependence of R on the reorientational correlation time (τ_c) in the region of the slow molecular motions, in which the small molecule is forced by the interaction with the cyclodextrin. In the fast-motion region ($\omega^2\tau_c^2 \ll 1$; ω = Larmor frequency), both the selective and nonselective relaxation rates increase progressively with increasing τ_c.[21] When the molecular motion of the ligand is slowed down to the $\omega^2\tau_c^2 \gg 1$ region as the consequence of the interaction with the host, R shows a sharp increase, whereas R^{ns} reaches a maximum for $\omega^2\tau_c^2 \cong 1$ and then decreases with further $\omega^2\tau_c^2$ increases. In the presence of well-resolved proton resonances, the selective relaxation rates can be easily determined by selective excitation of only one spin, leaving unperturbed the other ones, and by following the magnetization recovery in the time.

In the fast-exchange limit, both parameters (P), that is, the diffusion coefficients and the selective relaxation rates, are the weighted average of the values in the bound (P_b) and free (P_f) states (Eq. 2):

$$P_{obs} = x_b P_b + x_f P_f \quad (2)$$

where x_b and x_f are the molar fractions of the bound and free species.

For the pure DC (100 mM) in the absence of complexing agents we measured the diffusion coefficient of 4.8×10^{-10} m^2 s^{-1} (Table 3) and the proton selective relaxation rates of the protons H-a, H-f and H-g (see numbering in Chart 1) were 0.30, 0.39 and 0.22 s^{-1} (Table 4), respectively. In the presence of the cyclodextrin (DC/β-CDSH = 4:1) only a small decrease of the diffusion coefficient to the value of 4.3×10^{-10} m^2 s^{-1} was detected. Taking into account that the diffusion coefficient is the weighted average of its value in the free and bound states (Eq. 2) and that the translational diffusion of DC is mainly controlled by the cyclodextrin, we could assume the diffusion coefficient of the bound DC equal to the diffusion coefficient of the cyclodextrin and, hence, the DC bound molar fraction of 20% was calculated from Eq. 3.

$$x_b = \frac{D_{obs} - D_f}{D_b - D_f} = \frac{D_{obs} - D_f}{D_{\beta CDSH} - D_f} \quad (3)$$

The proton selective relaxation rates increased to the values of 2.16, 2.14 and 1.43 s^{-1} for the protons H-a, H-f and H-g, respectively, which pointed out about a six-fold increase of the NMR parameter (see normalized $\Delta R/R$ in the Table 4).

The solution of $(Au)_n$/β-CDSH nanoparticles which contains monomer cyclodextrin (3.7 mg/mL of metal and a five molar excess of the cyclodextrin with respect to the metal) was very stable during the time and no oxidation/precipitation occurred. Thus, the nanoparticles solution (25 mM in cyclodextrin) was added to DC (DC/β-CDSH = 4:1) and the NMR parameters were measured. The diffusion coefficient remarkably lowered to the value of 3.5×10^{-10} m^2 s^{-1} (Table 3). Thus, a very high bound molar fraction of 40% was obtained from Eq. 3 (using an averaged diffusion coefficient for β-CDSH of 1.3×10^{-10} m^2 s^{-1}). Relaxation measurements confirmed the enhanced ability of the cyclodextrin in the capped gold nanoparticles to bind the deoxycytidine, in fact a ten-fold increase of the proton selective relaxation rates was detected (Table 4), in agreement with the high complexation degree.

It is noteworthy that ROE measurements in the mixture DC/$(Au)_n$/β-CDSH NPs pointed to the occurrence of inclusion phenomena as several dipolar interactions were detected between DC protons and the protons H-3 and H-5 of the cyclodextrin, which were located in the inner part of the cyclodextrin.

Finally, starting from the more concentrated gold–acetone solution (3.7 mg/mL of metal), β-GluSNa-capped metal nanoparticles were isolated by adding a five molar excess of the ligand and easily re-dissolved in water. Hence the monosaccharide was able to bind the metal, which was confirmed also by the relevant broadening of the NMR resonances of the β-GluSNa due to the presence of the metal. In order to probe the ability of the corresponding water soluble nanoparticles to bind DC, the solution containing the β-GluSNa-capped gold nanoparticles was added to a four molar excess of DC. Both the selective relaxation rates and the diffusion coefficient of DC (Tables 3 and 4) were measured in order to detect their eventual perturbations due to the presence of the nanoparticles. However both kinds of NMR parameters remained nearly unchanged as in the presence of pure β-GluSNa (Tables 3 and 4).

The potentialities of the MVS technique for a very fine control of the gold nanoparticles sizes were confirmed, which was exploited in aqueous environment by the use of heptakis(6-deoxy-6-thio)cyclomaltoheptaose as the nanoparticles ligand by virtue of the high sulfur to gold affinity. A very useful procedure was developed, where the addition of the cyclodextrin to acetone-solvated nanoparticles led to the precipitation of cyclodextrin-bound gold nanoparticles, which were easily re-dissolved in water. The procedure not only was very simple, but also the use of potential chemical contaminants was avoided.

At high gold/cyclodextrin molar ratios, the oxidation of the cyclodextrin was favoured and under these conditions smaller nanoparticles were selected irrespective of the gold concentration in the starting Au/acetone SMA solution, probably due to the fact that the disulfide bridges have a lower affinity to gold than that the thiol groups bound to monomer cyclodextrin have. Furthermore the oxidized cyclodextrin has lower solubility which quicken the nanoparticles precipitation. This last feature intrinsically limits the use of gold nanoparticles to very diluted solutions. By contrast, in the solutions containing high molar excesses of the cyclodextrin to gold, only monomer cyclodextrin was present and the sizes of the gold aggregates could be modulated by means of the concentration of the solvated gold atoms coming from the MVS reactor. Such kinds of cyclodextrin-capped soluble nanoparticles are very suitable for the complexation of guests. The deoxycytidine was complexed with very good affinity by inclusion in spite of the fact that the original truncated cone shape of the cyclodextrin was strongly perturbed as the consequence of the metal complexation to the primary thiolated sites. The high degree of structural preorganization determined by the cyclic assembly of the glucopyranose units of the cyclodextrin and the occurrence of inclusion phenomena played a fundamental role in guests complexation processes. Accordingly, the 1-thio-β-D-glucose sodium salt, which was by itself able to bind and stabilize the gold and which led to the formation of water soluble gold nanoparticles, however, did not demonstrate any ability to act as a complexing agent for the deoxycytidine as in the case of the cyclodextrin.

Table 3
Diffusion coefficients (D, $\times 10^{10}$ m^2 s^{-1}, D_2O, 600 MHz, 25 °C) of DC alone (100 mM, D^{free}) and in mixture with β-CDSH or $(Au)_n$/β-CDSH NPs or β-GluSNa or $(Au)_n$/β-GluSNa NPs (complexing agent/DC = 1:4). Calculated bound molar fractions (x_b)

	DC	β-CDSH + DC	$(Au)_n$/β-CDSH NPs + DC	β-GluSNa + DC	$(Au)_n$/β-GluSNa NPs + DC
D	4.8	4.3	3.5	4.8	4.6
x_b		0.2	0.4	/	/

Table 4
Selective relaxation rates (R, s^{-1}, D_2O, 600 MHz, 25 °C) and normalized selective relaxation rate variations ($\Delta R/R$, $\Delta R = R^{mix} - R$) of selected protons of DC alone (100 mM, R) and in mixture (R^{mix}, complexing agent/DC = 1:4) with β-CDSH or $(Au)_n$/β-CDSH NPs or $(Au)_n$/β-GluSNa NPs

	DC	β-CDSH + DC		$(Au)_n$/β-CDSH NPs + DC		$(Au)_n$/β-GluSNa NPs + DC	
	R	R^{mix}	$\Delta R/R$	R^{mix}	$\Delta R/R$	R^{mix}	$\Delta R/R$
H-a	0.30	2.16	6.20	3.45	10.50	0.31	0.03
H-f	0.39	2.14	4.49	3.81	8.77	0.43	0.10
H-g	0.22	1.43	5.50	3.05	12.86	0.23	0.05

3. Experimental

3.1. General methods

The $(Au)_n$/β-CDSH NPs solid obtained following the above described procedure was dissolved in D_2O (0.7 mL) and then the dark-purple solution was transferred into a NMR tube under nitrogen atmosphere. NMR measurements were performed on a spectrometer operating at 600 and 150 MHz for ^1H and ^{13}C, respectively. The temperature was controlled to ±0.1 °C. The 2D NMR spectra were obtained by use of standard sequences and employing the minimal spectral width in both dimensions. g-COSY (gradient-COrrelation SpectroscopY) maps were acquired with a relaxation delay of 2 s and 2–4 scans of 256 increments each were collected. 2D TOCSY (TOtal Correlation SpectroscopY) spectra were recorded acquiring 2–4 scans with 256 increments, 2 K data points, 2 s relaxation delay and a mixing time of 80 ms. The gradient ^1H,^{13}C-HSQC (Heteronuclear Single Quantum Correlation) maps were obtained in 16 transients of 128 increments, with a relaxation delay of 1 s. The 2D ROESY (Rotating-frame Overhauser Enhancement SpectroscopY) spectra were recorded in the phase-sensitive mode, with a mixing time of 300 ms. The pulse delay was maintained at 5 s; 256 increments of 4 scans and 2 K data points were collected. Proton 1D ROESY spectra were recorded by using selective pulses generated by the Varian Pandora Software. The selective 1D ROESY spectra were acquired with 64 scans in 32 K data points with a 3 s relaxation delay and a mixing time of 0.3 s. DOSY (Diffusion Ordered SpectroscopY) experiments were carried out by using a stimulated echo sequence with self-compensating gradient schemes, the minimal spectral width and 64 K data points. The values of Δ and of δ were optimized for each sample and g was varied in 30 steps to obtain an approximately 90–95% decrease in resonance intensity at the largest gradient amplitudes. The baselines of all arrayed spectra were corrected prior to processing the data. After data acquisition, each FID was apodized with 1.0 Hz line-broadening and Fourier transformed. The data were processed with the DOSY macro (involving the determination of the resonance heights of all the signals above a pre-established threshold and the fitting of the decay curve for each resonance to a Gaussian function) to obtain pseudo-two-dimensional spectra with NMR chemical shifts along one axis and calculated diffusion coefficients along the other. The selective relaxation rates were measured in the initial rate approximation[22] by employing a selective π-pulse at the selected frequency. After the delay τ, a non-selective $\pi/2$ pulse was employed to detect the longitudinal magnetization.

3.2. Materials

1-Thio-β-D-glucose sodium salt (β-GluSNa) and all other reagents, except heptakis(6-deoxy-6-iodo)cyclomaltoheptaose (CycloLab), were from Sigma–Aldrich and were used without any additional purification. TLC plates were from Merck, type 5554 Silica Gel 60 F254. All the operations involving the use and the preparation of the solvated metal atoms (SMAs) were performed under dry argon atmosphere. Acetone was purified by conventional methods, distilled and stored under argon. Gold pellets (99.999%) were purchased from Chimet S.p.A.

3.3. Heptakis(6-deoxy-6-thiuronium)cyclomaltoheptaose heptaiodide (modified method of Rojas et al.)[23]

Dried heptakis(6-deoxy-6-iodo)cyclomaltoheptaose (14.3 g, 0.0075 mol) was dissolved in DMF (85 mL), approx. 15 mL of DMF was removed under reduced pressure and dried thiourea (8.0 g, 0.105 mol) was added at room temperature and heated up to 80 °C. The reaction mixture was stirred for 3 h at 80 °C, then cooled to 40 °C and the major part of DMF was removed under reduced pressure at 40 °C. The obtained crude product was recrystallized several times from 96% EtOH (100 mL). The obtained orange coloured product (13.1 g, 75%) was free from thiourea and was found to be appropriate for further reactions. RF = 0.35–0.40 10:7 dioxane/cc. NH_3.

3.4. Heptakis(6-deoxy-6-thio)cyclomaltoheptaose (modified method of Rojas et al.)[23]

The thiuronium salt (12.2 g, 0.005 mol) was heated around 100 °C in deoxygenated (He/ultrasound) 0.25 M NaOH (120 mL) for 4 h. As the reaction was completed the reaction mixture was cooled to around 5–10 °C and the pH was adjusted to 1.0–1.5 with 3 M HCl solution, when the product started to crystallize. As the pH became stable, the suspension was allowed to crystallize for 15 min, the solids were removed by filtration, washed with deoxygenated deionized water to around pH 5-6, then dried in vacuo at rt in the presence of P_2O_5 and KOH, and yielded 6.5 g of dark orange, glassy crystals. The obtained product was recrystallized by dissolution in deoxygenated 1 M NaOH solution (12 mL) and precipitated with 1 M HCl (18 mL). Filtration and washing to neutral pH with deoxygenated water afforded 3.8 g (61% theor.) light orange crystals. RF = 0.00–0.05 10:7 dioxane/cc. NH_3.

3.5. Regeneration of thiol group from its oxidized state

Partially oxidized heptakis(6-deoxy-6-thio)cyclomaltoheptaose (6.2 g, approx. 0.010 mol) was suspended in deoxygenated water and deoxygenated (He/ultrasound) 3 M NaOH solution (30 mL) was added at rt. Sodium borohydride (1.1 g, 0.030 mol) is added and stirred overnight. The occasionally found solids were filtered through a sintered glass funnel, the filtrate was cooled with an ice-water bath and the pH was adjusted to around 1.5–2 with 3 M HCl solution (approx. 45 mL). Upon acidification the product started to crystallize, and as the pH became stable and foaming stopped, the suspension was allowed to crystallize for an additional 15 min. The product was removed by filtration and washed to pH 5–7 with deoxygenated deionized water, then dried in vacuo at rt in the presence of P_2O_5 and KOH, yielded 3.2 g (∼50%) β-CDSH as a yellowish substance.

^1H NMR (D_2O, 25 °C): δ (ppm) 5.03 (H-1, d, $J_{1,2}$ 3.6 Hz, 7H), 3.83 (H-3, dd, $J_{3,2}$ 10.1 Hz, $J_{3,4}$ 9.3 Hz, 7H), 3.83 (H-5, m, 7H), 3.62 (H-4, dd, $J_{4,3} = J_{4,5}$ = 9.3 Hz, 7H), 3.52 (H-2, dd, $J_{2,3}$ 10.1 Hz, $J_{2,1}$ 3.6 Hz, 7H), 2.94 (H-6, d, $J_{6,6'}$ 13.6 Hz, 7H), 2.83 (H-6′, dd, $J_{6',6}$ 13.6 Hz, $J_{6',5}$ 4.8 Hz, 7H). ^{13}C NMR (D_2O, 25 °C): δ (ppm) 101.5 (C-1), 82.5 (C-4), 72.9 (C-3/C-5), 72.3 (C-2), 26.0 (C-6).

3.6. $(Au)_n$/β-CDSH NPs from LC Au/acetone SMA

In a typical experiment a portion of low concentrated (LC, 0.4 mg Au/mL) Au/acetone SMA (11.8 mL, 0.024 mmol Au) obtained as previously described in the literature[17] was added to a solution of β-CDSH in water (5 mL). The mixture was then stirred at rt and in the dark for about 30 min. During this period it was observed the formation of a dark-purple solid which was isolated and dried under reduced pressure. To obtain the samples containing different Au/β-CDSH ratio different amounts of β-CDSH were used: 150 mg (Au/β-CDSH = 1:5); 30 mg (Au/β-CDSH = 1:1) and 10 mg (Au/β-CDSH = 1:0.3).

$(Au)_n$/β-CDSH NPs (Au/β-CDSH = 1:5): ^1H NMR (D_2O, 25 °C): δ (ppm) 5.03 (H-1, d, $J_{1,2}$ 3.1 Hz, 7H), 3.80 (H-3, dd, $J_{3,2}$ 9.8 Hz, $J_{3,4}$ 9.3 Hz, 7H), 3.78 (H-5, m, 7H), 3.68 (H-4, dd, $J_{4,3} = J_{4,5}$ = 9.3 Hz, 7H), 3.50 (H-2, dd, $J_{2,3}$ 9.8 Hz, $J_{2,1}$ 3.1 Hz, 7H), 2.86 (H-6, dd, $J_{6,6'}$ 13.6 Hz, $J_{6,5}$ 2.8 Hz, 7H), 2.81 (H-6′, br d, $J_{6'6}$ 13.6 Hz, 7H).

3.7. $(Au)_n$/β-CDSH NPs from HC Au/acetone SMA

In a typical experiment a portion of high concentrated (HC, 3.7 mg Au/mL) Au/acetone SMA (1.3 mL, 0.024 mmol Au) was added to a solution of β-CDSH in water (2 mL). The mixture was then stirred at rt and in the dark for about 30 min and 10 mL of acetone was added to the mixture to facilitate the formation of a dark-purple precipitate which was isolated and dried under reduced pressure. To obtain the samples containing different Au/β-CDSH ratio different amounts of β-CDSH were used: 150 mg (Au/β-CDSH = 1:5); 30 mg (Au/β-CDSH = 1:1); 10 mg (Au/β-CDSH = 1:0.3) and 6 mg (Au/β-CDSH = 1:0.2).

3.8. $(Au)_n$/β-GluSNa NPs from Au/acetone SMA

2.8 mL (0.052 mmol Au) of high concentrated (HC, 3.7 mg Au/mL) Au/acetone SMA was added to a cooled solution (ice bath) of β-GluSNa in water (2 mL). The mixture was stirred at rt for about 1 h and then left over night to facilitate the formation of a dark-purple precipitate which was isolated and dried under reduced pressure. To obtain a sample containing 1:5 Au/β-GluSNa ratio 58 mg of β-GluSNa were used.

^{1}H NMR (D_2O, 25 °C): δ (ppm) 4.40 (H-1, br d, $J_{1,2}$ 6.2 Hz, 1H), 3.72 (H-6, d, $J_{6,6'}$ 12.7 Hz, 1H), 3.53 (H-6′, dd, $J_{6',6}$ 12.7 Hz, $J_{6',5}$ 4.6 Hz, 1H), 3.29-3.27 (H-3/H-4/H-5, m, 3H), 2.88 (H-2, dd, $J_{2,1} = J_{2,3}$ = 6.2 Hz, 1H).

Acknowledgements

The work was supported by the MIUR (FIRB Project RBPR05NWWC).

References

1. Brust, M.; Walker, M.; Bethell, D.; Schiffrin, D. J.; Whyman, R. *J. Chem. Soc., Chem. Commun.* **1994**, *7*, 801–802.
2. Daniel, M. C.; Astruc, D. *Chem. Rev.* **2004**, *104*, 293–346.
3. Katz, E.; Willner, I. *Angew. Chem., Int. Ed.* **2004**, *43*, 6042–6108.
4. Schmid, G. In *Cluster and Colloids: From Theory to Applications*; VCH: New York, 1994.
5. *Nanotechnology in Catalysis*; Ziou, B., Hermans, S., Somorjai, G. A., Eds.; Springer: New York, 2004.
6. Boisselier, E.; Astruc, D. *Chem. Soc. Rev.* **2009**, *38*, 1759–1782.
7. De, M.; Ghosh, P. S.; Rotello, V. M. *Adv. Mater.* **2008**, *20*, 4225–4241.
8. Kim, C. K.; Ghosh, P.; Rotello, V. M. *Nanoscale* **2009**, *1*, 61–67.
9. Murphy, C. J.; Gole, A. M.; Stone, J. W.; Sisco, P. N.; Alkilany, A. M.; Goldsmith, E. C.; Baxter, S. C. *Acc. Chem. Res.* **2008**, *41*, 1721–1730.
10. Rosi, N. L.; Mirkin, C. A. *Chem. Rev.* **2005**, *105*, 1547–1562.
11. Grabar, K. C.; Freeman, R. G.; Hommer, M. B.; Natan, M. J. *Anal. Chem.* **1995**, *67*, 735–743.
12. Liu, J.; Mendoza, S.; Roman, E.; Lynn, M. J.; Xu, R. L.; Kaifer, A. E. *J. Am. Chem. Soc.* **1999**, *121*, 4304–4305.
13. Liu, J.; Alvarez, J.; Kaifer, A. E. *Adv. Mater.* **2000**, *12*, 1381–1383.
14. Park, C.; Youn, H.; Kim, H.; Noh, T.; Kook, Y. H.; Oh, E. T.; Park, H. J.; Kim, C. *J. Mater. Chem.* **2009**, *19*, 2310–2315.
15. Klabunde, K. J. In *Free Atoms, Clusters and Nanoscale Particles*; Academic Press: San Diego, 1994.
16. Vitulli, G.; Evangelisti, C.; Caporusso, A. M.; Pertici, P.; Panziera, N.; Bertozzi, S.; Salvadori, P. Metal vapour-derived nanostructured catalysts in fine chemistry: the role played by particle size in the catalytic activity and selectivity In *Metal Nanoclusters in Catalysis, Materials Science. The Issue of Size-Control*; Corain, B., Schmid, G., Toshima, N., Eds.; Elsevier: Amsterdam, 2007. Chapter 32.
17. Aronica, A.; Schiavi, E.; Evangelisti, C.; Caporusso, A. M.; Salvadori, P.; Vitulli, G.; Bertinetti, L.; Martra, G. *J. Catal.* **2009**, *266*, 250–257.
18. Evangelisti, C.; Raffa, P.; Balzano, F.; Uccello-Barretta, G.; Vitulli, G.; Salvadori, P. *J. Nanosci. Nanotechnol.* **2008**, *8*, 2096–2101.
19. Uccello-Barretta, G.; Evangelisti, C.; Raffa, P.; Balzano, F.; Nazzi, S.; Martra, G.; Vitulli, G.; Salvadori, P. *J. Organomet. Chem.* **2009**, *694*, 1813–1817.
20. Hostetler, M. J.; Wingate, J. E.; Zhong, C. J.; Harris, J. E.; Vachet, R. W.; Clark, M. R.; Londono, J. D.; Green, S. J.; Stokes, J. J.; Wignall, G. D.; Glish, G. L.; Porter, M. D.; Evans, N. D.; Murray, R. W. *Langmuir* **1998**, *14*, 17–30.
21. Gaggelli, E.; Lepri, A.; Marchettini, N.; Ulgiati, S. Selective ^{1}H NMR Relaxation Delineation of Receptor Binding Equilibria In *Advanced Magnetic Resonance Techniques in Systems of High Molecular Complexity*; Niccolai, N., Valensin, G., Eds.; Birkhauser: Boston, 1986; pp 109–117.
22. Freeman, R.; Wittekoek, S. *J. Magn. Reson.* **1969**, *1*, 238–276.
23. Rojas, M. T.; Koeniger, R.; Stoddart, J. F.; Kaifer, A. E. *J. Am. Chem. Soc.* **1995**, *117*, 336–343.